

## RESEARCH ARTICLE

# Effects of Ferromagnetic Nanoparticles and Fluorination on Breakdown of SiR/Fe<sub>3</sub>O<sub>4</sub> Nanocomposites in High Magnetic Field

MINGYANG WANG<sup>1</sup>, YAO ZHANG<sup>1</sup>, CONGZHAO XUE<sup>1</sup>, BOXUE DU<sup>2</sup>, (Senior Member, IEEE), AND YUNQI XING<sup>3</sup>, (Member, IEEE)

<sup>1</sup>State Grid Tianjin High Voltage Company, Tianjin 300000, China

<sup>2</sup>School of Electrical and Information Engineering, Tianjin University, Tianjin 300000, China

<sup>3</sup>Key Laboratory of Electromagnetic Field and Electrical Apparatus Reliability of Hebei Province, Hebei University of Technology, Tianjin 300000, China

Corresponding author: Mingyang Wang (mywang@tju.edu.cn)

**ABSTRACT** High magnetic field causes premature failure of insulation. In order to improve the breakdown strength of silicone rubber (SiR), different filler contents of ferroferric oxide (Fe<sub>3</sub>O<sub>4</sub>) nanoparticles were added. Experimental results show that 1 wt% addition amount of ferromagnetic nanoparticles is beneficial to improve the AC breakdown strength of SiR by 5.40% in 12 T magnetic field due to their ability to regulate dielectric polarization and partial discharge (PD) behavior, resulting from the relative higher permittivity and permeability of Fe<sub>3</sub>O<sub>4</sub>. Magnetization of Fe<sub>3</sub>O<sub>4</sub> nanoparticles results in 3.33% decrease of DC breakdown strength with 2 wt% filler content in 12 T magnetic field. Fluorination treatment was carried out and proved to be able to improve the DC breakdown strength of SiR/Fe<sub>3</sub>O<sub>4</sub> nanocomposites by 8.84% in 12 T magnetic field with the treatment time being 5 minutes, resulting from the regulation of surface traps. Fluorination treatment weakened the magnetism of nanoparticles, weakening their regulation on insulation polarization and PD. Adding an appropriate amount of ferromagnetic nanoparticles before the fluorination of SiR/Fe<sub>3</sub>O<sub>4</sub> nanocomposites can improve the AC and DC breakdown strength by 0.64% and 8.81% respectively at the same time in high magnetic field.

**INDEX TERMS** High magnetic field, nanocomposites, fluorination treatment, polarization, insulation breakdown.

## I. INTRODUCTION

With the development of high-field magnets, it plays an important role in the fields of magnetic confinement nuclear fusion [1], [2], [3]. The reliability of coil insulation directly affects the safe and stable operation of the device and the stability of the entire system [4]. The heat shrinkable insulation represented by silicone rubber has been proved to be a feasible way for coil insulation [5]. While the operation of high-field magnets, the coil insulation faces the challenge of high magnetic field [6], [7]. As for the Central Solenoid (CS) coils in International Thermonuclear Experimental Reactor (ITER), the maximum magnetic flux density reaches 12 T [8]. Moreover, the coil insulation will withstand both steady

and transient high voltage when the magnet is in pulse current mode, with the current in the coil increasing and decreasing at uniform and variable rates [9]. Breakdown of coil insulation under the coupling effects of high magnetic field and strong electric field will cause significant economic losses and hinder the development of controllable nuclear fusion technology [4], [10]. According to technical standards, the processed coil insulation shall pass DC and AC tests [11], [12], without considering the effects of high magnetic field.

High magnetic field has been proved to be able to cause variation of dielectric properties [13] and promote partial discharge, deterioration [13], [14], [15], and breakdown [16] process of insulation material. Effects of high magnetic field on the electrons of polymer molecular chain result in energy level splitting, which is known as Zeeman effects [17]. Splitting of trap levels causes the decrease of energy barrier

The associate editor coordinating the review of this manuscript and approving it for publication was Giovanni Angiulli<sup>1</sup>.

during the hopping migration of charge carriers, resulting in the increase of DC conductivity [14]. Splitting of surface trap levels changes the D-value of the density of donor-like and acceptor-like traps, resulting in the decrease of interface barrier [16]. The larger amount of charge injection and space charge accumulation in high magnetic field increases the possibility of partial discharge (PD) and results in lower DC breakdown strength of insulation material [16]. The conversion between electromagnetic energy and dielectric polarization energy in high magnetic field leads to the variation of dielectric polarization process [13]. Inhibition effects on polarization cause lower amplitude and higher speed of polarization [13], [14], [15], resulting in the decrease of calculated permittivity and the increase of PD frequency in high magnetic field. As a result, electrical trees are more easily to be initiated and spread quickly toward the ground in insulation material under AC voltage [14], [15], [16]. Thus AC breakdown strength is decreased due to high magnetic field.

Experimental results and mechanism analysis in current research prove that the effects of high magnetic field cause the problem of lower AC and DC breakdown strength of insulation material, which remains unsolved based on the existing research and must be taken into account in the insulation design and factory acceptance testing of high-field magnets. Adding moderate contents of ferromagnetic nanoparticles to polymers has been proved to be a feasible way to resist the electrical treeing deterioration in gradient magnetic field [18]. The experimental result provides a possible method to resist insulation degradation. However, absence of research on mechanism of ferromagnetic particles affecting behavior of insulation material results in no theoretical guidance for improving AC breakdown strength. Modification method of adding surface functionalized nanoparticles is proved to be able to suppress the polarization of polymer insulation material due to the boundary between nanoparticles and polymer matrix. PD activity is also reduced due to nanoparticles' suppressing free space charges [19], [20]. Regarding the existing research, lack of research on improving AC and DC breakdown strength in high magnetic field simultaneously also handles the progress of insuring insulation reliability.

In this paper, adding  $\text{Fe}_3\text{O}_4$  nanoparticles, whose relative permittivity and permeability are higher than that of SiR, and fluorination treatments were carried out based on the mechanism of AC and DC breakdown in high magnetic field respectively. The mechanism of improving the breakdown strength by the modification methods was analyzed through experimental results and model calculations. The experimental results and the mechanism analysis provide a proper modification method to ensure insulation reliability in high magnetic and theoretical basis for the insulation design of high-field magnets.

## II. EXPERIMENTAL SETUP

### A. SPECIMEN PREPARATION

The specimens used in this paper are made of 110-2 methyl vinyl silicone rubber produced by Nanjing Dongjue

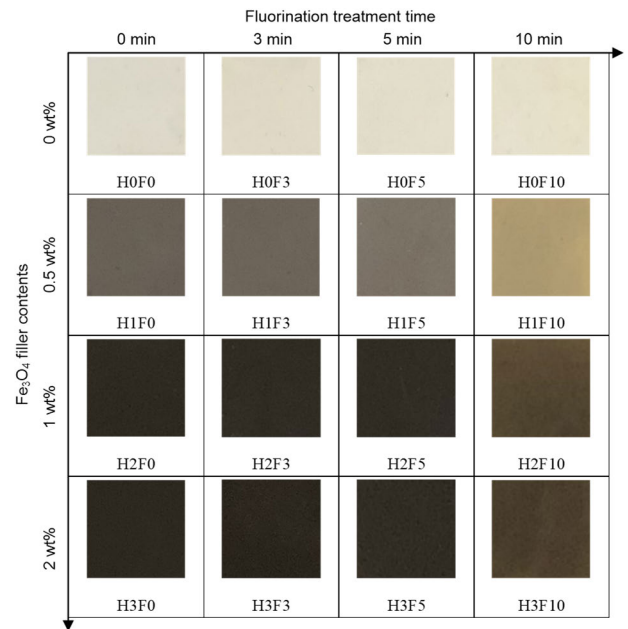


**FIGURE 1.** Pictures of the surface of specimens with different filler contents and fluorination time.

Silicone Co., Ltd., 2,5-dimethyl-2,5-bis(tert-butylperoxy) hexane (DBPH) sulfidizing agent produced by Guangdong Wengjiang Chemical Reagent Co., Ltd. and  $\text{Fe}_3\text{O}_4$  nanoparticles with an average grain diameter of 20 nm [18]. The silicone rubber and the sulfidizing agent were mixed in a mass ratio of 100:1. Then the  $\text{Fe}_3\text{O}_4$  nanoparticles were added to the mixture with contents of 0, 0.5, 1, 2 wt%. The three raw materials are mixed in corresponding proportions by a double screw blender at a speed of 120 rpm for half an hour. Then the material was extruded into a mold made of stainless steel and shaped into 60 mm×60 mm sheets with the thickness of 0.3 mm through hot pressing by setting the temperature and pressure as 175 °C and 10 MPa respectively for 20 minutes [21], forming sheets made of original SiR and SiR/ $\text{Fe}_3\text{O}_4$  nanocomposites.

In the process of fluorination treatment, the original SiR specimens and SiR/ $\text{Fe}_3\text{O}_4$  nanocomposites were suspended in the reactor by an iron bracket wrapped with polyimide. The temperature in the reactor was remained at 25 °C. Before the fluorination treatment, the reactor was vacuumed with a vacuum pump, then filled with nitrogen to atmospheric pressure, and then vacuumed again. The above process was repeated three times to complete gas washing. After the gas washing stage, the reactor was filled with fluorine gas to half atmospheric pressure [22] and the fluorination reaction was carried out, which lasts for 3, 5 and 10 minutes respectively. After the fluorination reaction, the process of vacuuming the reactor and filling the reactor with nitrogen is repeated for three times again to complete the gas washing stage.

The pictures of the surface of the specimens used in this paper with the color of the background being white are shown in Fig. 1. The specimens with different contents of  $\text{Fe}_3\text{O}_4$  nanoparticles and being fluorinated for different times are

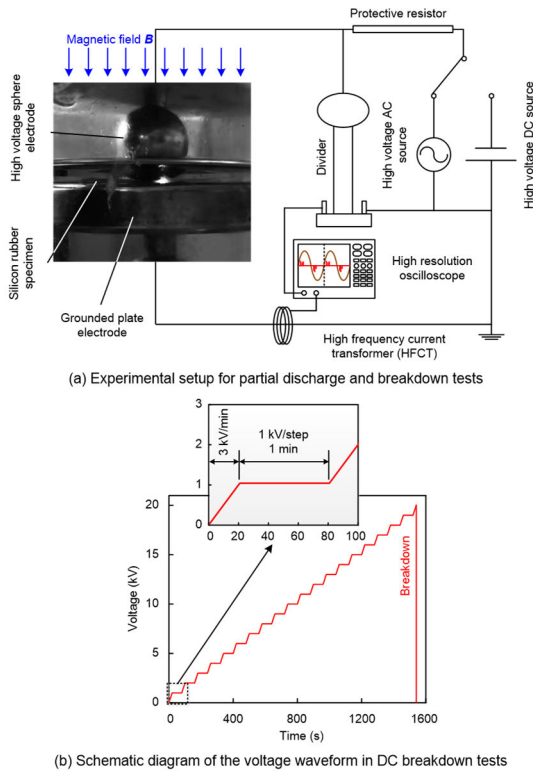


**FIGURE 2.** Experimental setup for partial discharge and breakdown tests as well as the voltage waveform in DC breakdown tests.

discriminated by the first half (H0, H1, H2 and H3) and the second half of the labels (F0, F3, F5 and F10) respectively.

### B. PARTIAL DISCHARGE AND BREAKDOWN TESTS

The experiments in this paper were all carried out at room temperature. High magnetic field was generated by a superconducting high-field magnet, JM-TD-12T100, with the largest magnetic flux density being over 12 T. The direction of external magnetic field is perpendicular to the surface of the specimens. AC and DC breakdown tests were carried out using the same sphere-plate electrode system made of brass as described in [16]. The diameter of the sphere electrode is 20 mm as shown in Fig. 2(a). During AC breakdown tests, the rising speed of the applied voltage is 3 kV/min. The applied voltage rises from 0 kV to the breakdown of the specimens, and the process is repeated 10 times for each type of specimen in each condition with different magnetic flux densities. During DC breakdown tests, step-up boosting method [16] was used, with the relationship between the voltage applied to the specimens and the time being described by the diagram in Fig. 2(b). Breakdown strengths of the specimens were calculated through dividing the breakdown voltage by the actual thickness of the sample measured with a vernier caliper.

PD behavior was tested using the same experimental setup as that used in AC breakdown tests and was detected by a high-frequency current transformer (HFCT) being connected to a high-resolution oscilloscope and surrounding the ground

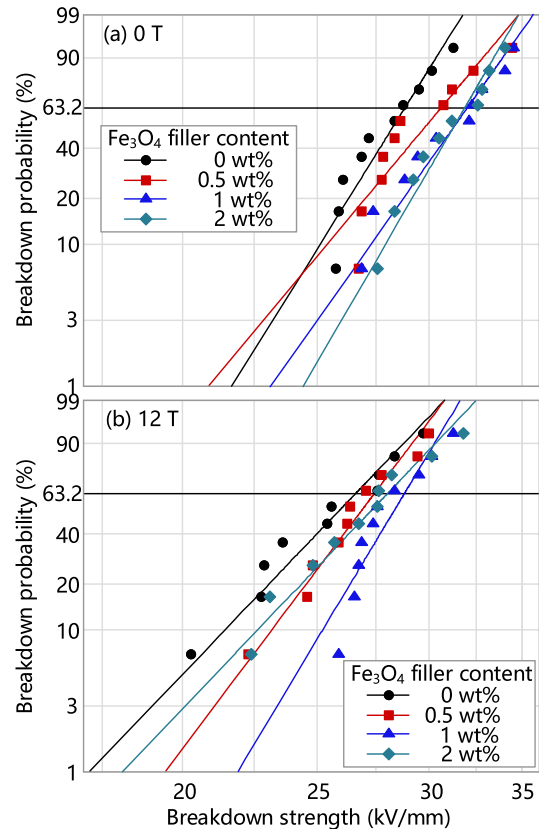


**FIGURE 3.** High magnetic field affecting AC breakdown strength of SiR/Fe<sub>3</sub>O<sub>4</sub> nanocomposites.

line as described in [13], [15], and [16]. 5 kV AC voltage was applied to the specimens for 1 minute, and PDs whose amplitudes of the signals were higher than 200 mV were recorded.

The surface density of different types of shallow traps on the specimens' surface was tested and calculated using the same experimental setup and equations respectively as described in [16]. The charging process lasts for 10 minutes, and the discharging process lasts for 20 minutes. Distributions of donor-like and acceptor-like surface shallow traps are tested with the voltage polarity of the needle electrode being positive and negative respectively.

## III. RESULTS AND DISCUSSION

### A. EFFECTS OF NANOPARTICLES ON BREAKDOWN

The AC breakdown strength of SiR/Fe<sub>3</sub>O<sub>4</sub> nanocomposites with different addition amounts of Fe<sub>3</sub>O<sub>4</sub> nanoparticles in situations without external magnetic field and with the magnetic flux density being 12 T is shown in Fig. 3. In a magnetic field free environment, the AC breakdown strength of the SiR composite insulation specimens with Fe<sub>3</sub>O<sub>4</sub> nanoparticles added is higher than that of the original SiR specimen, and the AC breakdown strength of the composite insulation specimens increases with the increase of the mass fraction of Fe<sub>3</sub>O<sub>4</sub> nanoparticles. AC breakdown strength of the composite specimens with the mass fractions of Fe<sub>3</sub>O<sub>4</sub> nanoparticles being 1 wt% and 2 wt% is almost the same.

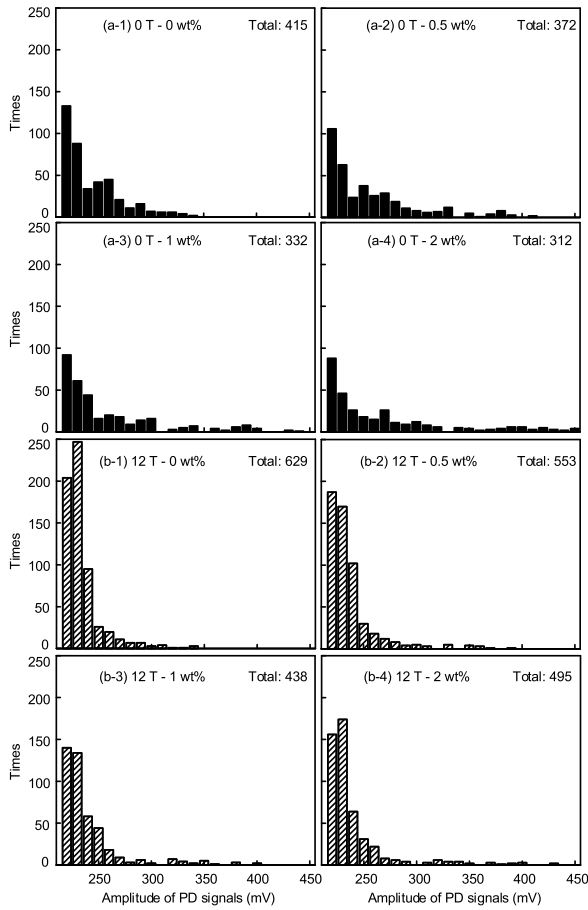


FIGURE 4. Statistical data of high magnetic field affecting PD amplitudes and times.

When the magnetic flux density is 12 T, the AC breakdown strength of SiR/Fe<sub>3</sub>O<sub>4</sub> nanocomposites is higher than that of the original SiR specimen. The AC breakdown strength is the highest when the mass fraction of Fe<sub>3</sub>O<sub>4</sub> nanoparticles is 1 wt%. The AC breakdown strength of the four types of specimens in high magnetic field is lower than that in free environment. Therefore, high magnetic field reduces the AC breakdown strength of SiR. Adding an appropriate amount of Fe<sub>3</sub>O<sub>4</sub> nanoparticles can effectively improve the AC breakdown strength of SiR in the absence of magnetic field and high magnetic field.

Under AC voltage, the change of breakdown strength is closely related to the behavior of PD. The damage of PD to the specimens develops rapidly from the specimens' surface to the ground electrode and finally penetrates the specimens to cause insulation breakdown. Statistical data of the amplitudes and times of PDs with the electrodes being applied with 5 kV AC voltage for 1 minute are shown in Fig. 4

As for the specimens with the same content of Fe<sub>3</sub>O<sub>4</sub> nanoparticles, the average amplitude of PDs decreases and more PDs take place in high magnetic field compared to that in the situation without external magnetic field. Higher PD frequency results in the decrease of AC breakdown strength in high magnetic field. In the situation without external

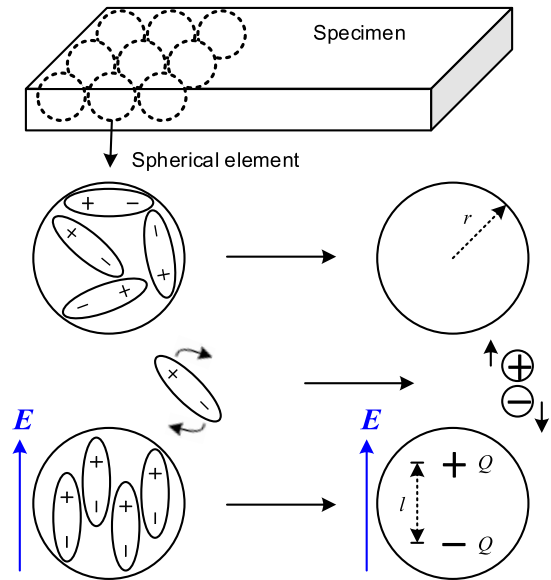


FIGURE 5. Schematic diagram of the model to calculate the effects of magnetic field on polarization.

magnetic field, the PD frequency decreases and average PD amplitude increases with the increase of filler contents. Coupling effects of lower PD frequency and higher average PD amplitude result in similar AC breakdown strength of the specimens with 1 and 2 wt% filler contents. In high magnetic field with the magnetic flux density being 12 T, PD frequency of the specimen with 2 wt% Fe<sub>3</sub>O<sub>4</sub> nanoparticles is higher than that with 1 wt% Fe<sub>3</sub>O<sub>4</sub> nanoparticles. Higher total discharge energy per unit time leads to a weaker inhibition effect on AC breakdown in high magnetic field with the contents of Fe<sub>3</sub>O<sub>4</sub> nanoparticles being higher than 1 wt%.

PD behaviors are related to the polarization and depolarization process of the polymer insulation material as described in [13] and [16]. In order to analyze the effects of high magnetic field on the dielectric properties of SiR/Fe<sub>3</sub>O<sub>4</sub> nanocomposites, a model is established and shown in Fig. 5.

One piece of a specimen can be divided into a finite number of spherical elements whose radius is *r*. The movement of all physical elements (electrons, ions, dipoles, et al.) taking part in polarization process is unified into the separation of positive and negative charge centers. As a result, the model is suitable for elements of all sizes. The spherical elements can represent both SiR matrix and Fe<sub>3</sub>O<sub>4</sub> nanoparticles. Considering the energy conversion in the range of spherical elements during the polarization of specimens, the conservation equation of energy density is as follows [13], [15], [16].

$$\frac{1}{2}\epsilon\epsilon_0E^2 + \frac{1}{2}\mu\mu_0H_0^2 = \frac{3JElt}{4\pi r^3\epsilon} + \frac{3\sqrt{\epsilon\mu}}{4c}E(H_0 + H) \quad (1)$$

where  $\epsilon$  and  $\mu$  are relative permittivity and permeability respectively;  $\epsilon_0$  and  $\mu_0$  are the permittivity and permeability of vacuum;  $E$  is the external electric field;  $H_0$  is the external magnetic field intensity;  $J$  is the current density generated by polarization;  $l$  is the length of electric dipole;  $c$  is the speed of



light;  $H$  is the magnetic field intensity generated by  $J$ . As a result, the electromagnetic field affecting dipole moment  $d(t)$  and the time for depolarization  $\tau$  can be expressed by the equations (2) and (3) respectively [13], [16].

$$d(t) = \frac{4\pi r^3}{3} \varepsilon^2 \varepsilon_0 E \left[ 1 - 1.5 \sqrt{\frac{\mu\mu_0}{\varepsilon\varepsilon_0}} \frac{H_0}{E} + \frac{\mu\mu_0}{\varepsilon\varepsilon_0} \left( \frac{H_0}{E} \right)^2 \right] \cdot \ln \left( \frac{lct}{\pi r^2 \sqrt{\varepsilon\mu}} + 1 \right) \quad (2)$$

$$\tau = \frac{\pi r^2}{2lc} \sqrt{\varepsilon\mu} \left[ 1 - \exp \left( -\frac{2lcQ_{\max}}{\pi r^3 H_0 \sqrt{\varepsilon\mu}} \right) \right] \quad (3)$$

where  $Q_{\max}$  is the quantity of polarized charges.

As for the specimens with the same contents of  $\text{Fe}_3\text{O}_4$  nanoparticles, higher magnetic flux density results in lower polarization intensity and higher speed of depolarization, causing higher PD frequency and lower average PD amplitude. SiR/ $\text{Fe}_3\text{O}_4$  nanocomposites display much higher permittivity and permeability than original SiR specimen. As a result, addition of appropriate amount of  $\text{Fe}_3\text{O}_4$  nanoparticles is able to arrange the polarization of SiR in the situations with high magnetic field and without external magnetic field, resulting in lower PD frequency and higher AC breakdown strength. Higher filler content (2 wt%) causes both higher PD frequency and higher average PD amplitude, resulting in lower AC breakdown strength in high magnetic field, due to the magnetization of  $\text{Fe}_3\text{O}_4$  nanoparticles.

**B. EFFECTS OF FLUORINATION ON DC BREAKDOWN**

The DC breakdown strength of fluorinated SiR specimens in situations with high magnetic field and without external magnetic field is shown in Fig. 6.

The DC breakdown strength of the specimens increases with the increase of fluorination treatment time, except for the specimen being fluorinated for 10 minutes. As for the specimens being fluorinated for the same time, high magnetic field causes the decrease of DC breakdown strength.

Scanning electron microscope (SEM) images of the fracture surface of the specimens are shown in Fig. 7. Fluorination treatment generates a fluorinated layer on the surface of the specimens. The thickness of the fluorinated layer increases with the increase of fluorination treatment time. Although the thickest fluorinated layer appears on the SiR specimen being fluorinated for 10 minutes, the fluorination treatment also causes damage to the specimen’s surface, resulting in the demonstrable decrease of DC breakdown strength.

According to [14] and [16], high magnetic field affects the charge injection barrier through splitting the energy levels of polymer insulation material and changing the surface density of the two types of surface traps. Lower charge injection barrier causes more space charge accumulation, resulting in the decrease of DC breakdown strength in high magnetic field [16]. Changes in the density of two types of surface traps after fluorination treatment in high magnetic field are shown in Fig. 8. Difference between the densities of donor-like and acceptor-like is calculated and marked at the corresponding

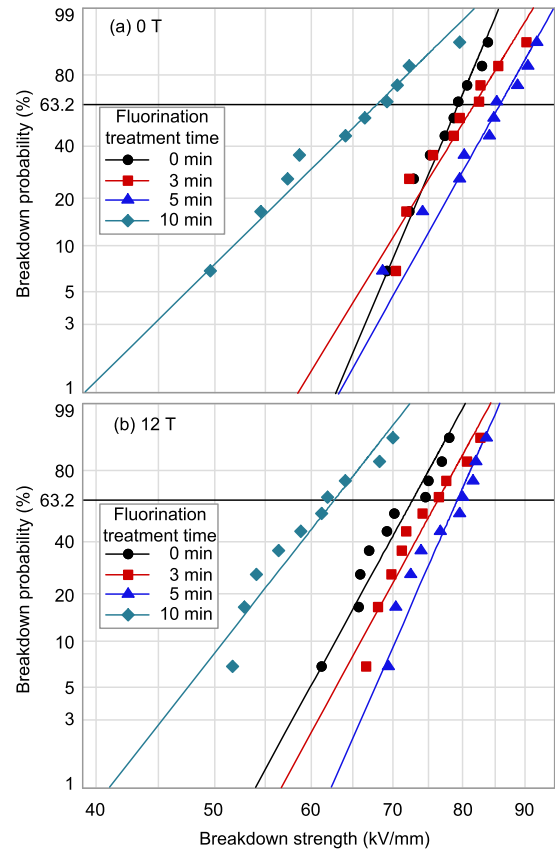


**FIGURE 6.** High magnetic field affecting DC breakdown strength of fluorinated SiR specimens.

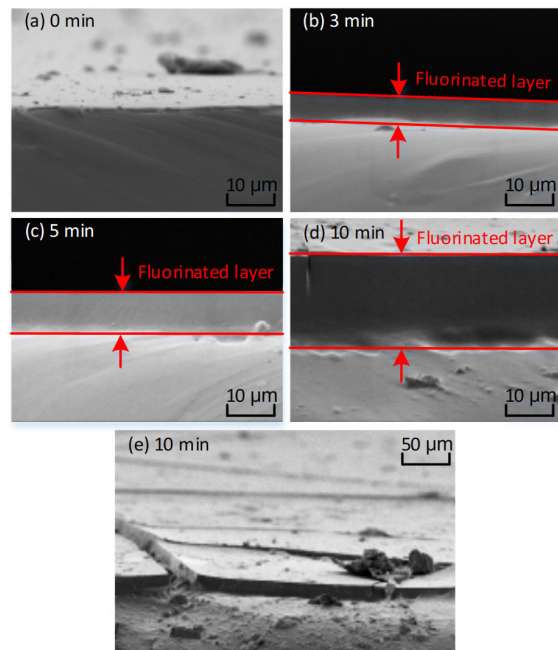


**FIGURE 7.** SEM images of the fracture surface of fluorinated SiR specimens.

position of each specimen. Compared with the original SiR specimens, fluorination treatment results in larger density of

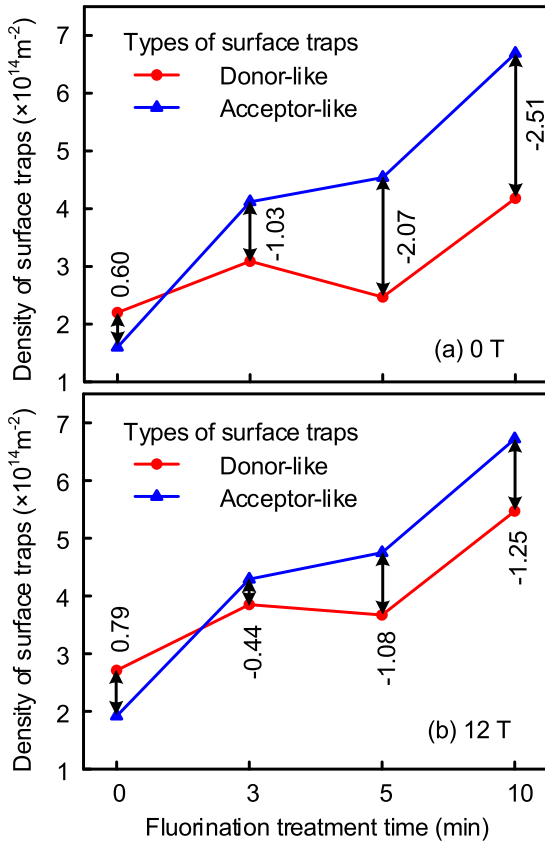


FIGURE 8. Changes in densities of surface traps by fluorination treatment time in high magnetic field.

acceptor-like surface traps, which is caused by electronegativity of the fluorinated layer. With the increase of magnetic flux density, both the densities of donor-like and acceptor-like surface traps increase. High magnetic field has more significant effects on the increase of donor-like surface trap density, resulting in lower density difference between the two types of surface traps with the magnetic flux density being 12 T. Higher surface density of acceptor-like traps is favorable for the improvement of interface barrier [16], resisting space charge injection and PD. As a result, fluorination treatment is able to increase the DC breakdown strength of SiR both in high magnetic field and conditions without magnetic field.

C. COLLABORATIVE REGULATION

Considering the fact that high-field magnet coil insulation faces the challenge of steady-state and transient high voltage simultaneously, DC breakdown tests on nanocomposites in high magnetic field were carried out to verify the universality of adding Fe<sub>3</sub>O<sub>4</sub> particles. Scale parameter of the Weibull distribution of DC breakdown strength of SiR/Fe<sub>3</sub>O<sub>4</sub> nanocomposites is shown in Fig. 9

While in the situation without magnetic field, DC breakdown strength increases with the increase of Fe<sub>3</sub>O<sub>4</sub> filler contents. The Fe<sub>3</sub>O<sub>4</sub> nanoparticles form quantum dots and play a role as deep traps [18]. Higher filler contents result in higher density of deep traps, capturing homo-polar charges

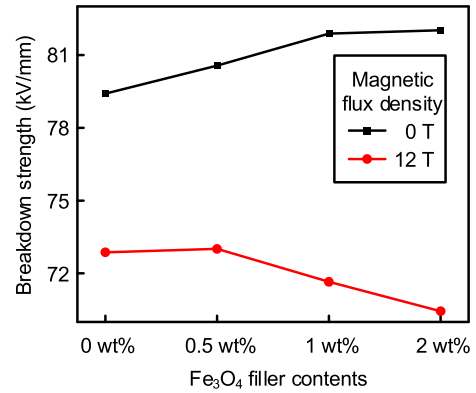


FIGURE 9. High magnetic field affecting DC breakdown strength of SiR/Fe<sub>3</sub>O<sub>4</sub> nanocomposites.

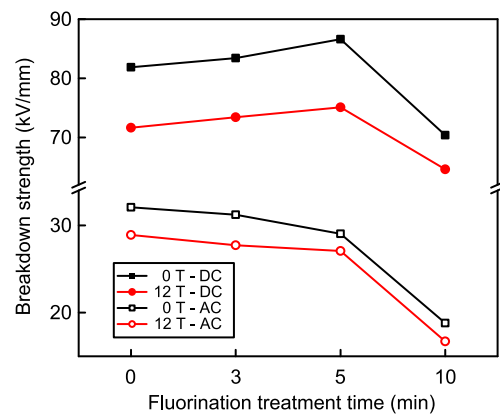


FIGURE 10. Magnetic field affecting DC and AC breakdown strength of fluorinated nanocomposites with 1 wt% filler content.

and resisting space charge injection, causing higher DC breakdown strength. While in high magnetic field, the magnetization of Fe<sub>3</sub>O<sub>4</sub> nanoparticles enlarges the effect of magnetic field on the reduction of interface barrier. As a result, adding Fe<sub>3</sub>O<sub>4</sub> nanoparticles fails in increasing DC breakdown strength of SiR in high magnetic field.

The SiR/Fe<sub>3</sub>O<sub>4</sub> nanocomposite with 1 wt% filler content, which shows the highest AC breakdown strength in high magnetic field, is fluorinated. AC and DC breakdown strength of the fluorinated nanocomposites in the condition without magnetic field and in high magnetic field is shown in Fig. 10

The nanocomposites being fluorinated for 5 minutes also show the highest DC breakdown strength with the magnetic flux density being 0 and 12 T. However, the AC breakdown strength decreases with the increase of fluorination treatment time. Besides the damage caused by overdose fluorination, fluorination treatment also weakens the effect of Fe<sub>3</sub>O<sub>4</sub> nanoparticles on improving the AC breakdown strength of SiR. The magnetic hysteresis loops of the fluorinated nanocomposites are shown in Fig. 11.

As a polymer, SiR is antimagnetic, thus the tail of magnetic hysteresis loops of the SiR/Fe<sub>3</sub>O<sub>4</sub> nanocomposites shows a downward trend. With the increase of fluorination treatment time, except 10 minutes, the magnetism of the

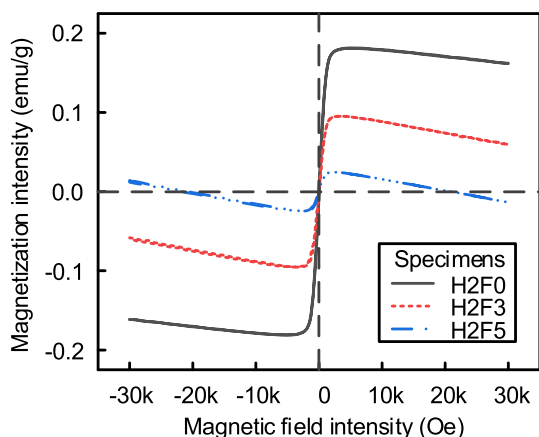


FIGURE 11. Magnetic hysteresis loops of the fluorinated nanocomposites (from 0 to 3 T).

TABLE 1. Specimens with the highest breakdown strength.

	DC breakdown		AC breakdown	
	0 T	12 T	0 T	12 T
0 wt%	H0F5	H0F5	H0F0	H0F0
0.5 wt%	H1F5	H1F5	H1F0	H1F0
1 wt%	H2F5	H2F5	H2F0	H2F0
2 wt%	H3F5	H3F5	H3F0	H3F5

TABLE 2. The highest breakdown strength of the specimens with the same filler content.

	DC breakdown strength (kV/mm)		AC breakdown strength (kV/mm)	
	0 T	12 T	0 T	12 T
0 wt%	85.94	79.31	28.90	26.67
0.5 wt%	86.24	77.50	30.72	27.49
1 wt%	86.60	75.11	32.07	28.90
2 wt%	87.02	73.34	31.93	29.02

SiR/Fe<sub>3</sub>O<sub>4</sub> nanocomposites is weakened. By combining the color of specimens shown in Fig. 1, conclusions can be drawn that fluorination treatment converts some of the magnetic Fe<sub>3</sub>O<sub>4</sub> nanoparticles into non-magnetic FeF<sub>2</sub> and FeF<sub>3</sub>, which are crystals with the color of light green. According to equations (2) and (3), lower permeability weakens the modification effects of nanoparticles on the polarization of SiR.

DC and AC breakdown tests on the specimens in Fig. 1 were carried out with the magnetic flux density being 0 and 12 T. The specimen with the highest breakdown strength and the corresponding breakdown strength are counted and shown in Table 1 and Table 2.

DC and AC breakdown strength of H0F0 is 79.41 and 28.90 kV/mm in the condition without magnetic field, and 72.87 and 26.67 kV/mm in high magnetic field, respectively. With the filler content being the same, all the specimens being fluorinated for 5 minutes show the highest DC breakdown strength, and all the specimens except those who have 2 wt% Fe<sub>3</sub>O<sub>4</sub> nanoparticles show the highest AC breakdown

strength when fluorination treatment is not carried out. Both DC and AC breakdown strength of H3F5 is higher than the original SiR specimen in high magnetic field. Considering the effects of fluorination treatment on the conversion of Fe<sub>3</sub>O<sub>4</sub> nanoparticles, H3F5 has a larger quantity of magnetic fillers left than H2F5 does. As a result, relative higher DC and AC breakdown strength of H3F5 in high magnetic field is caused by a) higher density of quantum dots, b) electronegative fluorinated layer and c) enough magnetic particles after fluorination treatment.

#### IV. CONCLUSION

This paper investigates the effects of adding Fe<sub>3</sub>O<sub>4</sub> nanoparticles and fluorination treatment on the AC and DC breakdown strength of SiR in high magnetic field respectively. The two modification methods are combined to improve the AC and DC breakdown strength of SiR simultaneously. Main conclusions are as follows:

(1) Fe<sub>3</sub>O<sub>4</sub> nanoparticles can modify the polarization of SiR and cause the decrease of PD frequency. As a result, adding 1 wt% Fe<sub>3</sub>O<sub>4</sub> nanoparticles can improve the AC breakdown strength of SiR in high magnetic field by 5.4%. Magnetization of Fe<sub>3</sub>O<sub>4</sub> nanoparticles makes the magnetic field more significant in promoting the breakdown of SiR with the filler content being excessive.

(2) Fluorination treatment generates a fluorinated layer on the surface of SiR and improves the density of acceptor-like surface traps. 5 minutes of fluorination treatment causes the increase of interface barrier and improves the DC breakdown strength of SiR in high magnetic field by 8.84%. Overdose fluorination treatment causes damage to SiR and results in a significant decrease in breakdown strength.

(3) Fe<sub>3</sub>O<sub>4</sub> nanoparticles act as quantum dots, resisting space charge injection and improving DC breakdown strength in the conditions without magnetic field. Magnetization of Fe<sub>3</sub>O<sub>4</sub> nanoparticles causes decrease of DC breakdown strength in high magnetic field.

(4) Fluorination treatment reduces the magnetism of Fe<sub>3</sub>O<sub>4</sub> nanoparticles, thus reducing the inhibitory effect of magnetic nanoparticles on AC breakdown. Through supplementing an appropriate amount of magnetic nanoparticles to SiR/Fe<sub>3</sub>O<sub>4</sub> nanocomposites, the combination of fluorination treatment and adding Fe<sub>3</sub>O<sub>4</sub> nanoparticles can improve the AC and DC breakdown strength in high magnetic field by 0.64% and 8.81% simultaneously.

Based on the experimental results and mechanism analysis in this paper, the structural design of coil insulation will be carried out in the future, completing a highly reliable insulation design for high-field magnets using the material preparation method obtained in this paper.

#### REFERENCES

[1] K. Li, Z. Y. Liu, Y. L. Yao, Z. H. Zhao, C. Dong, D. Li, S. P. Zhu, X. T. He, and B. Qiao, "Modification of the fusion energy gain factor in magnetic confinement fusion due to plasma temperature anisotropy," *Nucl. Fusion*, vol. 62, no. 8, Aug. 2022, Art. no. 086026.

- [2] D. Perrault, "Nuclear safety aspects on the road towards fusion energy," *Fusion Eng. Design*, vol. 146, pp. 130–134, Sep. 2019.
- [3] D. C. van der Laan, K. Radcliff, V. A. Anvar, K. Wang, A. Nijhuis, and J. D. Weiss, "High-temperature superconducting CORC<sup>®</sup> wires with record-breaking axial tensile strain tolerance present a breakthrough for high-field magnets," *Superconductor Sci. Technol.*, vol. 34, no. 10, Oct. 2021, Art. no. 10LT01.
- [4] W. Lee, D. Park, J. Bascunan, and Y. Iwasa, "Partial-insulation HTS magnet for reduction of quench-induced peak currents," *IEEE Trans. Appl. Supercond.*, vol. 32, no. 6, pp. 1–5, Sep. 2022.
- [5] H. Hu, Z. Jia, and X. Wang, "Aging mechanism of silicone rubber under thermal–tensile coupling effect," *IEEE Trans. Dielectr. Electr. Insul.*, vol. 29, no. 1, pp. 185–192, Feb. 2022.
- [6] M. Y. Wang, B. X. Du, X. T. Han, and Z. L. Li, "Effects of magnetic field on partial discharge in epoxy resin for superconducting coil insulation," *IEEE Trans. Appl. Supercond.*, vol. 31, no. 8, pp. 1–3, Nov. 2021.
- [7] Y. Xing, Y. Wang, Y. Shen, B. Wang, and Z. Guo, "Electrical tree characteristics of epoxy resin under lightning impulse at cryogenic temperature," *IEEE Trans. Dielectr. Electr. Insul.*, vol. 29, no. 5, pp. 1721–1726, Oct. 2022.
- [8] T. Bagni, M. Breschi, S. Jagga, and A. Devred, "Calculation method for pulsed magnetic field energy supplied to Nb<sub>3</sub>Sn ITER CS conductors during SULTAN stability tests," *Fusion Eng. Des.*, vol. 147, Oct. 2019, Art. no. 111224.
- [9] Y. Bi, Z. Zhang, Y. Chen, D. Chen, H. Zhou, Z. Jin, and X.-F. Li, "A pulsed current charging mechanism for high temperature superconducting magnets," *IEEE Trans. Appl. Supercond.*, vol. 32, no. 4, pp. 1–5, Jun. 2022.
- [10] B. X. Du, M. M. Zhang, T. Han, and J. G. Su, "Tree initiation characteristics of epoxy resin in Ln<sub>2</sub> for superconducting magnet insulation," *IEEE Trans. Dielectr. Electr. Insul.*, vol. 22, no. 4, pp. 1793–1800, Aug. 2015.
- [11] G. Kim, S. H. Park, J. Bang, C. Im, J. Kim, J. Yoon, K. J. Han, S. Noguchi, and S. Hahn, "Experimental study and frequency domain analysis on metal-insulation HTS coil," *IEEE Trans. Appl. Supercond.*, vol. 32, no. 4, pp. 1–5, Jun. 2022.
- [12] Y. Ma, H. Han, H. Jin, D. Yin, Y. Wu, H. Liu, and Y. Hu, "Electrical insulation testing for CFETR CS model coil," *IEEE Trans. Appl. Supercond.*, vol. 31, no. 5, pp. 1–4, Aug. 2021.
- [13] M. Wang, B. Du, X. Kong, H. Liang, and Y. Ma, "High magnetic field affecting dielectric polarization and partial discharge behavior of epoxy resin," *IEEE Trans. Dielectr. Electr. Insul.*, vol. 29, no. 4, pp. 1267–1274, Aug. 2022.
- [14] M. Y. Wang, B. X. Du, X. X. Kong, Z. L. Li, M. Xiao, and Y. W. Ma, "Effects of gradient magnetic field on charge behavior and electrical tree growth in epoxy resin," *IEEE Trans. Dielectr. Electr. Insul.*, vol. 28, no. 5, pp. 1686–1693, Oct. 2021.
- [15] M. Y. Wang, B. X. Du, X. T. Han, X. X. Kong, Z. L. Li, and M. Xiao, "Effects of high magnetic field on partial discharge and flashover behavior of epoxy resin," *IEEE Trans. Dielectr. Electr. Insul.*, vol. 31, no. 8, Nov. 2020.
- [16] M. Wang, B. Du, X. Kong, Z. Li, T. Han, and Y. Ma, "Effects of high magnetic field on partial discharge and dielectric breakdown behavior of silicone rubber," *IEEE Trans. Dielectr. Electr. Insul.*, vol. 29, no. 3, pp. 915–923, Jun. 2022.
- [17] S. Sun, Z. D. Song, H. M. Weng, and X. Dai, "Topological metals induced by the Zeeman effect," *Phys. Rev. B, Condens. Matter*, vol. 101, no. 12, Mar. 2020, Art. no. 125118.
- [18] M. Y. Wang, B. X. Du, X. X. Kong, and T. Tanaka, "Effects of ferromagnetism particles on electrical tree growth in epoxy/Fe<sub>3</sub>O<sub>4</sub> composites in magnetic field," *IEEE Trans. Dielectr. Electr. Insul.*, vol. 28, no. 4, pp. 1291–1299, Aug. 2021.
- [19] N. M. K. Abdel-Gawad, A. Z. El Dein, D. A. Mansour, H. M. Ahmed, M. M. F. Darwish, and M. Lehtonen, "Development of industrial scale PVC nanocomposites with comprehensive enhancement in dielectric properties," *IET Sci., Meas. Technol.*, vol. 13, no. 1, pp. 90–96, Jan. 2019.
- [20] N. M. K. Abdel-Gawad, A. Z. El Dein, D. A. Mansour, H. M. Ahmed, M. M. F. Darwish, and M. Lehtonen, "PVC nanocomposites for cable insulation with enhanced dielectric properties, partial discharge resistance and mechanical performance," *High Voltage*, vol. 5, no. 4, pp. 463–471, Aug. 2020.
- [21] E. Cho, L. L. Y. Chiu, M. Lee, D. Naila, S. Sadanand, S. D. Waldman, and D. Sussman, "Characterization of mechanical and dielectric properties of silicone rubber," *Polymers*, vol. 13, no. 11, p. 1831, Jun. 2021.
- [22] Y. Mai, B. Du, Y. Zhao, Q. Liu, and W. Yang, "Modulation of epoxy polymer trapping energy levels by fluorinated diluents to improve insulation properties," *IEEE Trans. Dielectr. Electr. Insul.*, vol. 29, no. 3, pp. 1062–1069, Jun. 2022.



**MINGYANG WANG** received the Ph.D. degree in electrical engineering from Tianjin University, in 2022. He is currently an Engineer with State Grid Tianjin High Voltage Company. He has published more than 30 articles in his research-related fields. His major research interests include insulation failure in the electromagnetic field, dielectric properties in an extreme environment, relay protection principles, and power system reliability.



**YAO ZHANG** received the M.S. degree from the Hebei University of Technology, Tianjin, China, in 2009. He is currently a Deputy Senior Engineer and a Senior Technician with State Grid Tianjin High Voltage Company. He has been engaged in the operation and maintenance management of substation equipment for a long time, with strong professional skills and rich on-site experience.



**CONGZHAO XUE** received the M.S. degree in electrical engineering from Beijing Jiaotong University, in 2022. He is currently with State Grid Tianjin High Voltage Company. His major research interests include lithium-ion battery energy storage technology and battery management systems.



**BOXUE DU** (Senior Member, IEEE) received the M.E. degree in electrical engineering from Ibaraki University, Hitachi, Japan, in 1993, and the Ph.D. degree from the Tokyo University of Agriculture and Technology, Tokyo, Japan, in 1996. From 1996 to 2002, he was with the Niigata Institute of Science and Technology, Niigata, Japan, and an Associate Professor. From 2000 to 2002, he was a Visiting Scientist with Niigata University, Niigata. Since 2002,

he has been a Professor and the Director-Founder with the Institute of High Voltage, School of Electrical and Information Engineering, Tianjin University, Tianjin, China. His research interests include advanced insulation materials for electrical equipment, polymer dielectrics for energy storage, and high-voltage insulation technology. He is a fellow of IET and a member of several working groups in the International Council on Large Electric Systems and several standards committees in IEEE. He has/had served as a guest editor/associate editor for a number of IEEE TRANSACTIONS and IET journals.



**YUNQI XING** (Member, IEEE) was born in Shandong, China, in 1986. He received the B.S. degree from the China University of Mining and Technology, Xuzhou, Jiangsu, China, in 2009, the M.S. degree from the Shandong University of Technology, Zibo, Shandong, in 2013, and the Ph.D. degree in electrical engineering from Tianjin University, Tianjin, China, in 2017. He is currently an Associate Professor with the School of Electrical Engineering, Hebei University of Technology, Tianjin. His current research interests include new dielectric materials, extreme environment insulation technology, and reliability improvement for GIS/GIL.

...